Study of electroweak $Z\gamma$ production in anomalous quartic gauge couplings

Artur Semushin

NRNU MEPhI

2022 March 23

EFT parameterization

$$\mathcal{L} = \mathcal{L}_{SM} + \sum_{d>4} \sum_i \frac{F_i^{(d)}}{\Lambda^{d-4}} \mathcal{O}_i^{(d)} = \mathcal{L}_{SM} + \sum_{d>4} \sum_i f_i^{(d)} \mathcal{O}_i^{(d)}. \quad (1)$$

- $f_i^{(d)} = \frac{F_i^{(d)}}{\Lambda^{d-4}} \quad [\text{TeV}^{-(d-4)}]$.
- The lowest operators dimension, which can be used for studying genuine aQGC, is $d = 8$.

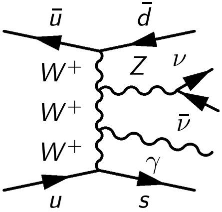

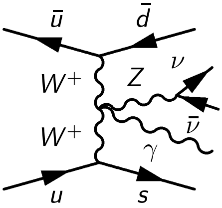

Construction of the operators

- $\hat{W}_{\mu\nu} = \frac{\sigma^i}{2} W^i_{\mu\nu}$,

where $W^i_{\mu\nu} = \partial_\mu W^i_\nu - \partial_\nu W^i_\mu + g\varepsilon^{ijk} W^j_\mu W^k_\nu$.

- $B_{\mu\nu} = \partial_\mu B_\nu - \partial_\nu B_\mu$.

- $D_\mu = \partial_\mu + ig\frac{\sigma_i}{2} W^i_\mu + ig'\frac{Y}{2} B_\mu$.

- $\Phi = \frac{v+H}{\sqrt{2}} \begin{pmatrix} 0 \\ 1 \end{pmatrix}$.

8-dimensional operators (genuine aQGC, Èboli basis)

$$\mathcal{O}_{\mathrm{S0}} = \left[(D_\mu \Phi)^\dagger D_\nu \Phi \right] \left[(D^\mu \Phi)^\dagger D^\nu \Phi \right],$$

$$\mathcal{O}_{\mathrm{S1}} = \left[(D_\mu \Phi)^\dagger D^\mu \Phi \right] \left[(D_\nu \Phi)^\dagger D^\nu \Phi \right].$$

$$\mathcal{O}_{\mathrm{M0}} = \mathrm{Tr} \left[\hat{W}_{\mu\nu} \hat{W}^{\mu\nu} \right] \left[(D_\beta \Phi)^\dagger D^\beta \Phi \right],$$

$$\mathcal{O}_{\mathrm{M1}} = \mathrm{Tr} \left[\hat{W}_{\mu\nu} \hat{W}^{\nu\beta} \right] \left[(D_\beta \Phi)^\dagger D^\mu \Phi \right],$$

$$\mathcal{O}_{\mathrm{M2}} = \left[B_{\mu\nu} B^{\mu\nu} \right] \left[(D_\beta \Phi)^\dagger D^\beta \Phi \right],$$

$$\mathcal{O}_{\mathrm{M3}} = \left[B_{\mu\nu} B^{\nu\beta} \right] \left[(D_\beta \Phi)^\dagger D^\mu \Phi \right],$$

$$\mathcal{O}_{\mathrm{M4}} = \left[(D_\mu \Phi)^\dagger \hat{W}_{\beta\nu} D^\mu \Phi \right] B^{\beta\nu},$$

$$\mathcal{O}_{\mathrm{M5}} = \left[(D_\mu \Phi)^\dagger \hat{W}_{\beta\nu} D^\nu \Phi \right] B^{\beta\mu} + \text{h.c.},$$

$$\mathcal{O}_{\mathrm{M7}} = \left[(D_\mu \Phi)^\dagger \hat{W}_{\beta\nu} \hat{W}^{\beta\mu} D^\nu \Phi \right].$$

$$\mathcal{O}_{\mathrm{T0}} = \mathrm{Tr} \left[\hat{W}_{\mu\nu} \hat{W}^{\mu\nu} \right] \mathrm{Tr} \left[\hat{W}_{\alpha\beta} \hat{W}^{\alpha\beta} \right],$$

$$\mathcal{O}_{\mathrm{T1}} = \mathrm{Tr} \left[\hat{W}_{\alpha\nu} \hat{W}^{\mu\beta} \right] \mathrm{Tr} \left[\hat{W}_{\mu\beta} \hat{W}^{\alpha\nu} \right],$$

$$\mathcal{O}_{\mathrm{T2}} = \mathrm{Tr} \left[\hat{W}_{\alpha\mu} \hat{W}^{\mu\beta} \right] \mathrm{Tr} \left[\hat{W}_{\beta\nu} \hat{W}^{\nu\alpha} \right],$$

$$\mathcal{O}_{\mathrm{T5}} = \mathrm{Tr} \left[\hat{W}_{\mu\nu} \hat{W}^{\mu\nu} \right] \left[B_{\alpha\beta} B^{\alpha\beta} \right],$$

$$\mathcal{O}_{\mathrm{T6}} = \mathrm{Tr} \left[\hat{W}_{\alpha\nu} \hat{W}^{\mu\beta} \right] \left[B_{\mu\beta} B^{\alpha\nu} \right],$$

$$\mathcal{O}_{\mathrm{T7}} = \mathrm{Tr} \left[\hat{W}_{\alpha\mu} \hat{W}^{\mu\beta} \right] \left[B_{\beta\nu} B^{\nu\alpha} \right],$$

$$\mathcal{O}_{\mathrm{T8}} = \left[B_{\mu\nu} B^{\mu\nu} \right] \left[B_{\alpha\beta} B^{\alpha\beta} \right],$$

$$\mathcal{O}_{\mathrm{T9}} = \left[B_{\alpha\mu} B^{\mu\beta} \right] \left[B_{\beta\nu} B^{\nu\alpha} \right].$$

Affected couplings

Operator	$WWWW$	$WWZZ$	$WWZ\gamma$	$WW\gamma\gamma$	$ZZZZ$	$ZZZ\gamma$	$ZZ\gamma\gamma$	$Z\gamma\gamma\gamma$	$\gamma\gamma\gamma\gamma$
$\mathcal{O}_{S0}$, $\mathcal{O}_{S1}$	○	○			○				
$\mathcal{O}_{T0}$, $\mathcal{O}_{T1}$, $\mathcal{O}_{T2}$	○	○	○	○	○	○	○	○	○
$\mathcal{O}_{T5}$, $\mathcal{O}_{T6}$, $\mathcal{O}_{T7}$		○	○	○	○	○	○	○	○
$\mathcal{O}_{T8}$, $\mathcal{O}_{T9}$					○	○	○	○	○
$\mathcal{O}_{M0}$, $\mathcal{O}_{M1}$, $\mathcal{O}_{M7}$	○	○	○	○	○	○	○		
$\mathcal{O}_{M2}$, $\mathcal{O}_{M3}$, $\mathcal{O}_{M4}$, $\mathcal{O}_{M5}$		○	○	○	○	○	○		

Amplitude decomposition

Parameterization by a single operator:
$\mathcal{L} = \mathcal{L}_{\text{SM}} + f\mathcal{O}$.

Squared amplitude:
$|\mathcal{A}|^2 = |\mathcal{A}_{\text{SM}} + f\mathcal{A}_{\text{BSM}}|^2 =$
$= |\mathcal{A}_{\text{SM}}|^2 + f2\text{Re}(\mathcal{A}^{\dagger}_{\text{SM}}\mathcal{A}_{\text{BSM}}) + f^2|\mathcal{A}_{\text{BSM}}|^2$

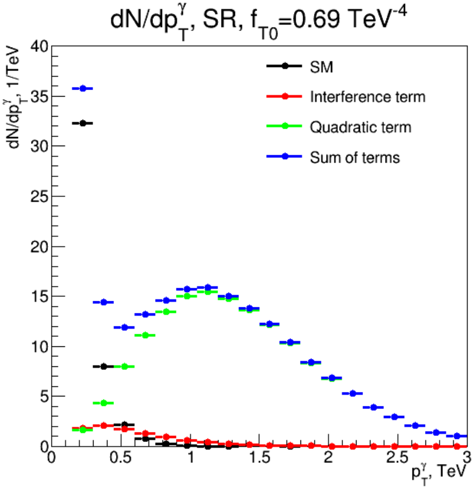

Unitarity violation and clipping

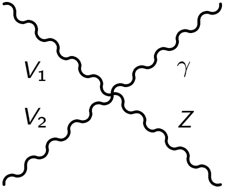

VBS: $\sqrt{s} = m_{Z\gamma}$.
S-matrix unitarity: $SS^{+} = 1$.
Usage of EFT violates unitarity.

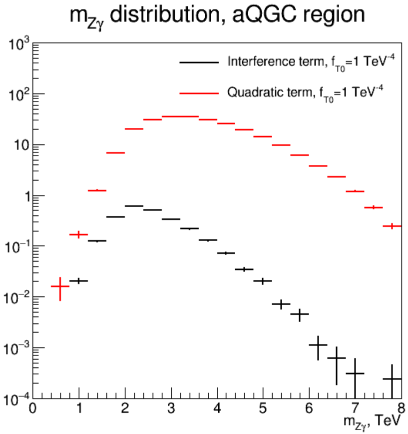

Clipping technique is dropping of new physics contributions with $\sqrt{s} > E_{\text{clip}}$.

Unitarity bounds

Simplified illustration for how unitarity bound can be calculated. $2 \to 2$ elastic VBS is considered. $\mathcal{A}$ — its amplitude.

Partial wave expansion: $\mathcal{A} = 16\pi \sum_J (2J+1) P_J(\cos\theta) A_J$. (1)

$2 \to 2$ differential cross section in the center of mass system: $\frac{d\sigma}{d\Omega} = \frac{|\mathcal{A}|^2}{64\pi^2 s}$. (2)

$\implies \sigma = \frac{16\pi}{s} \sum_J (2J+1)|A_J|^2$. (3)

Another way: unitarity condition $SS^\dagger = 1$ leads to optical theorem:

$\sigma_{\text{tot}} = \frac{1}{s} \operatorname{Im} \mathcal{A}(\theta = 0)$. (4)

$(3) \leq (4) \implies |A_J|^2 \leq \operatorname{Im} A_J \implies |A_J|^2 \leq 1$ and $|A_J| < 1$.

Phase space optimization

Example: optimization for f_{T0}.

E_{clip}, TeV	∞	1.8	1.7	1.6
p_T^γ>150 GeV	[-0.62; 0.58]	[-2.1; 1.8]	[-2.3; 1.9]	[-2.6; 2.2]
p_T^γ>300 GeV	[-0.36; 0.32]	[-1.24; 1]	[-1.4; 1.1]	[-1.6; 1.2]
p_T^γ>400 GeV	[-0.26; 0.23]	[-0.94; 0.75]	[-1.06; 0.83]	[-1.22; 0.95]
p_T^γ>500 GeV	[-0.21; 0.19]	[-0.81; 0.65]	[-0.93; 0.74]	[-1.08; 0.86]
p_T^γ>600 GeV	[-0.18; 0.16]	[-0.76; 0.63]	[-0.89; 0.73]	[-1.06; 0.87]
p_T^γ>700 GeV	[-0.16; 0.14]	[-0.78; 0.67]	[-0.94; 0.81]	[-1.2; 1]
p_T^γ>800 GeV	[-0.14; 0.13]	[-0.87; 0.77]	[-1.07; 0.96]	[-1.4; 1.2]
p_T^γ>900 GeV	[-0.13; 0.12]	[-1.02; 0.94]	[-1.3; 1.2]	[-1.6; 1.5]
p_T^γ>1000 GeV	[-0.12; 0.12]	[-1.3; 1.2]	[-1.6; 1.6]	[-2.1; 2]
p_T^γ>1100 GeV	[-0.12; 0.12]			
p_T^γ>1200 GeV	[-0.12; 0.11]			
p_T^γ>1300 GeV	[-0.13; 0.12]			
Bound	[-0.0; 0.0]	[-0.72; 0.72]	[-0.9; 0.9]	[-1.2; 1.2]

Optimization result

Chosen regions:

For non-unitarized limits:
$p_T^\gamma > 900$ GeV.

For unitarized limits:

- $p_T^\gamma > 600$ GeV for T-family;
- $p_T^\gamma > 400$ GeV for M-family.

Results for f_{T0}

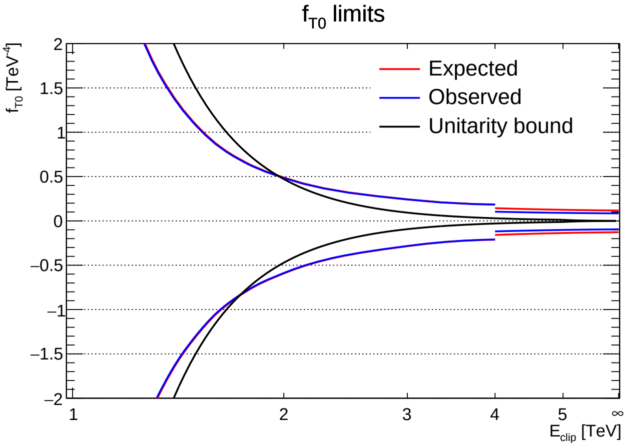

<u>Non-unitarized limits.</u>

Expected: [-0.13; 0.12] TeV^{-4}.

Observed: [-0.095; 0.085] TeV^{-4}.

<u>Unitarized limits.</u>

$E_{clip} = 1.7$ TeV.

Expected: [-0.89; 0.73] TeV^{-4}.

Observed: [-0.88; 0.72] TeV^{-4}.

Linear limits: introduction

Usual case (with quadratic term):

$$\mathcal{A} = \mathcal{A}_{\text{SM}} + \frac{F}{\Lambda^4}\mathcal{A}_{\text{BSM}} \to |\mathcal{A}|^2 = |\mathcal{A}_{\text{SM}}|^2 + \frac{F}{\Lambda^4} 2\text{Re}\left(\mathcal{A}^{\dagger}_{\text{SM}}\mathcal{A}_{\text{BSM}}\right) + \frac{F^2}{\Lambda^8}|\mathcal{A}_{\text{BSM}}|^2$$

- F^{real} and $f^{\text{real}} = \dfrac{F^{\text{real}}}{\Lambda^4}$ are actual values of EFT couplings.
- $F^{\text{real}} \ll 1$, $\Lambda \gg$ modern experiments energy scale.

$\Longrightarrow$ quadratic term can be dropped.

Example of f_{T0}:

- $N \approx 45 + 14 f_{\text{T0}} + 330 f^2_{\text{T0}}$ — predicted number of events in the SR, no clipping.
- Limit value: $f^{\text{limit}}_{\text{T0}} \approx 0.1\ \text{TeV}^{-4} \Longrightarrow$ int. and quad. terms: 1.4 and 3.3 — are the same order.
- $f^{\text{real}}_{\text{T0}} \ll f^{\text{limit}}_{\text{T0}} \Longrightarrow$ quad. term is much smaller than int. term.

Linear limits: theoretical limit

Model without quadratic term (linear model):

$|\mathcal{A}|^2 = |\mathcal{A}_{\mathrm{SM}}|^2 + f\,2\mathrm{Re}\left(\mathcal{A}_{\mathrm{SM}}^{\dagger}\mathcal{A}_{\mathrm{BSM}}\right) \geq 0, \quad \mathcal{A}_{\mathrm{SM}} = \mathcal{A}_{\mathrm{EWK}} + \mathcal{A}_{\mathrm{QCD}}$

$\implies N = N_{\mathrm{SM}} + fN_{\mathrm{int}} \geq 0$ — predicted number of events.

This condition leads to theoretical constraint on f:

$$N_{\mathrm{int}} > 0 \rightarrow f_{\mathrm{min}} = -\frac{N_{\mathrm{SM}}}{N_{\mathrm{int}}},$$

$$N_{\mathrm{int}} < 0 \rightarrow f_{\mathrm{max}} = -\frac{N_{\mathrm{SM}}}{N_{\mathrm{int}}}$$

Linear limits: optimization

Since statistical uncertainty on the interference term is significant in the strict phase space regions (especially for M-family), theoretical limit inherits this uncertainty. Regions with too large statistical uncertainty on theoretical limit was not considered on the optimization procedure to ensure constant sign of the theoretical limit.

Regions chosen after optimization:

- $p_{\mathrm{T}}^{\gamma} > 800$ GeV for T-family;
- $p_{\mathrm{T}}^{\gamma} > 400$ GeV for M-family.

Linear limits: results

Coef.	Expected limits, TeV^{-4}	Observed limits, TeV^{-4}
f_{T0}	[-0.36; 1.38]	[-0.36; 0.88]
f_{T5}	[-1.37; 0.35]	[-0.87; 0.35]
f_{T8}	[-35; 136]	[-35; 86]
f_{T9}	[-53; 208]	[-53; 132]
f_{M0}	[-870; 850]	[-1110; 670]
f_{M1}	[-2800; 2800]	[-2200; 3600]
f_{M2}	[-420; 430]	[-330; 540]

BACK-UP

Calculation of the unitarity bound

Considered process: $V_{1,\lambda_1} V_{2,\lambda_2} \to V_{3,\lambda_3} V_{4,\lambda_4}$.

Partial-wave expansion of the amplitude:

$$\mathcal{A} = 16\pi \sum_J (2J+1) \sqrt{1+\delta^{V_{2,\lambda_2}}_{V_{1,\lambda_1}}} \sqrt{1+\delta^{V_{4,\lambda_4}}_{V_{3,\lambda_3}}} d^J_{\lambda\mu}(\theta) e^{iM\varphi} T^J. \quad (1)$$

Partial-wave unitarity requirement: $|T^J| \leq 1$.

States in helicity particle space with fixed partial wave J and charge Q were considered in the analysis. Example: $Q = 2,\ J = 0 \Longrightarrow$ basis $(W^+_+ W^+_+, W^+_0 W^+_0, W^+_- W^+_-)$.

$$T^0 = \frac{1}{96\pi} \frac{s^2}{\Lambda^4} \begin{pmatrix} 6f_{T1} + 3f_{T2} & 0 & 4f_{T0} + 8f_{T1} + f_{T2} \\ 0 & 3f_{S0} + f_{S1} + f_{S2} & 0 \\ 4f_{T0} + 8f_{T1} + f_{T2} & 0 & 6f_{T1} + 3f_{T2} \end{pmatrix}. \quad (2)$$

Partial-wave unitarity requirement is used for all eigenvalues of this matrix.

Unitarity bound: results

Coefficient	1 operator	All operators
$\lvert\frac{f_{T0}}{\Lambda^4}\rvert$	$\frac{12}{5}\pi s^{-2}$	$\frac{136}{11}\pi s^{-2}$
$\lvert\frac{f_{T8}}{\Lambda^4}\rvert$	$\frac{3}{2}\pi s^{-2}$	$\frac{18}{5}\pi s^{-2}$
$\lvert\frac{f_{M0}}{\Lambda^4}\rvert$	$\frac{32}{\sqrt{6}}\pi s^{-2}$	$\frac{2}{3}(72+5\sqrt{6})\pi s^{-2}$
$\lvert\frac{f_{M1}}{\Lambda^4}\rvert$	$\frac{128}{\sqrt{6}}\pi s^{-2}$	$8(24+\frac{\sqrt{6}}{5})\pi s^{-2}$
$\lvert\frac{f_{S0}}{\Lambda^4}\rvert$	$32\pi s^{-2}$	$48\pi s^{-2}$
$\lvert\frac{f_{S1}}{\Lambda^4}\rvert$	$\frac{96}{7}\pi s^{-2}$	$\frac{288}{5}\pi s^{-2}$

- The main advantage of these bounds — they are analytical.
- Only leading unitarity-violated term of the amplitude was taken into account ($\propto s^2$).
- Minimal scenario gives tighter and more correct bounds than the second scenario.

f_{T5} optimization [1]

E_{clip}, TeV	∞	5	4	3	2.9	2.8
p_T^γ>150 GeV	[-0.61; 0.65]	[-0.64; 0.69]	[-0.7; 0.77]	[-0.89; 0.99]	[-0.92; 1.03]	[-0.96; 1.07]
p_T^γ>300 GeV	[-0.34; 0.38]	[-0.35; 0.4]	[-0.39; 0.44]	[-0.5; 0.58]	[-0.51; 0.6]	[-0.54; 0.63]
p_T^γ>400 GeV	[-0.24; 0.27]	[-0.25; 0.29]	[-0.28; 0.32]	[-0.36; 0.42]	[-0.37; 0.44]	[-0.39; 0.46]
p_T^γ>500 GeV	[-0.19; 0.22]	[-0.2; 0.23]	[-0.23; 0.26]	[-0.29; 0.35]	[-0.3; 0.36]	[-0.32; 0.38]
p_T^γ>600 GeV	[-0.16; 0.19]	[-0.17; 0.2]	[-0.19; 0.22]	[-0.25; 0.3]	[-0.27; 0.31]	[-0.28; 0.33]
p_T^γ>700 GeV	[-0.15; 0.16]	[-0.15; 0.17]	[-0.17; 0.2]	[-0.23; 0.27]	[-0.24; 0.28]	[-0.26; 0.3]
p_T^γ>800 GeV	[-0.13; 0.15]	[-0.14; 0.16]	[-0.16; 0.18]	[-0.22; 0.25]	[-0.23; 0.26]	[-0.24; 0.28]
p_T^γ>900 GeV	[-0.12; 0.13]	[-0.13; 0.14]	[-0.15; 0.17]	[-0.22; 0.24]	[-0.23; 0.26]	[-0.25; 0.28]
p_T^γ>1000 GeV	[-0.12; 0.13]	[-0.13; 0.14]	[-0.15; 0.16]	[-0.23; 0.25]	[-0.25; 0.27]	[-0.27; 0.29]
p_T^γ>1100 GeV	[-0.12; 0.13]	[-0.13; 0.14]	[-0.15; 0.17]	[-0.25; 0.27]	[-0.27; 0.29]	[-0.3; 0.32]
p_T^γ>1200 GeV	[-0.12; 0.13]	[-0.13; 0.14]	[-0.16; 0.17]	[-0.28; 0.3]		
p_T^γ>1300 GeV	[-0.13; 0.14]	[-0.14; 0.15]	[-0.18; 0.19]	[-0.36; 0.37]		
Bound	[-0; 0]	[-0.023; 0.023]	[-0.057; 0.057]	[-0.18; 0.18]	[-0.21; 0.21]	[-0.24; 0.24]

f_{T5} optimization [2]

E_{clip}, TeV	2.7	2.6	2.5	2.4	2.3	2.2	2.1
p_T^γ>150 GeV	[-1; 1.1]	[-1; 1.2]	[-1.1; 1.2]	[-1.2; 1.3]	[-1.2; 1.4]	[-1.3; 1.5]	[-1.4; 1.6]
p_T^γ>300 GeV	[-0.56; 0.66]	[-0.58; 0.69]	[-0.61; 0.73]	[-0.65; 0.78]	[-0.69; 0.83]	[-0.73; 0.89]	[-0.78; 0.96]
p_T^γ>400 GeV	[-0.4; 0.49]	[-0.42; 0.51]	[-0.45; 0.54]	[-0.47; 0.58]	[-0.5; 0.62]	[-0.54; 0.67]	[-0.58; 0.72]
p_T^γ>500 GeV	[-0.33; 0.4]	[-0.35; 0.42]	[-0.37; 0.45]	[-0.39; 0.48]	[-0.42; 0.52]	[-0.45; 0.56]	[-0.49; 0.61]
p_T^γ>600 GeV	[-0.29; 0.35]	[-0.31; 0.37]	[-0.33; 0.39]	[-0.35; 0.43]	[-0.38; 0.46]	[-0.41; 0.5]	[-0.45; 0.55]
p_T^γ>700 GeV	[-0.27; 0.32]	[-0.29; 0.34]	[-0.31; 0.36]	[-0.33; 0.4]	[-0.36; 0.43]	[-0.4; 0.48]	[-0.44; 0.53]
p_T^γ>800 GeV	[-0.26; 0.3]	[-0.28; 0.32]	[-0.3; 0.35]	[-0.33; 0.38]	[-0.36; 0.42]	[-0.41; 0.47]	[-0.46; 0.53]
p_T^γ>900 GeV	[-0.26; 0.3]	[-0.29; 0.32]	[-0.31; 0.35]	[-0.35; 0.39]	[-0.39; 0.44]	[-0.45; 0.51]	[-0.53; 0.59]
p_T^γ>1000 GeV	[-0.29; 0.32]	[-0.32; 0.35]	[-0.36; 0.39]	[-0.41; 0.45]	[-0.47; 0.52]	[-0.56; 0.61]	[-0.67; 0.72]
p_T^γ>1100 GeV	[-0.33; 0.36]	[-0.38; 0.41]	[-0.43; 0.46]	[-0.51; 0.54]	[-0.6; 0.64]	[-0.72; 0.77]	[-0.86; 0.91]
p_T^γ>1200 GeV							
p_T^γ>1300 GeV							
Bound	[-0.27; 0.27]	[-0.32; 0.32]	[-0.37; 0.37]	[-0.44; 0.44]	[-0.52; 0.52]	[-0.62; 0.62]	[-0.75; 0.75]

Results for f_{T5}

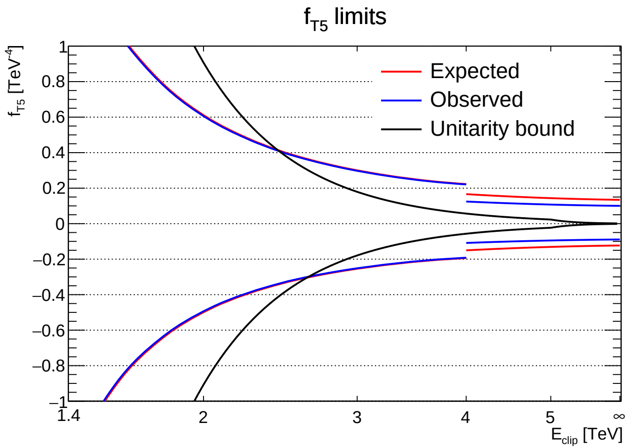

<u>Non-unitarized limits.</u>

Expected: [-0.12; 0.13] TeV^{-4}.

Observed: [-0.089; 0.100] TeV^{-4}.

<u>Unitarized limits.</u>

$E_{\text{clip}} = 2.4$ TeV.

Expected: [-0.35; 0.43] TeV^{-4}.

Observed: [-0.35; 0.42] TeV^{-4}.

Results for f_{T8}

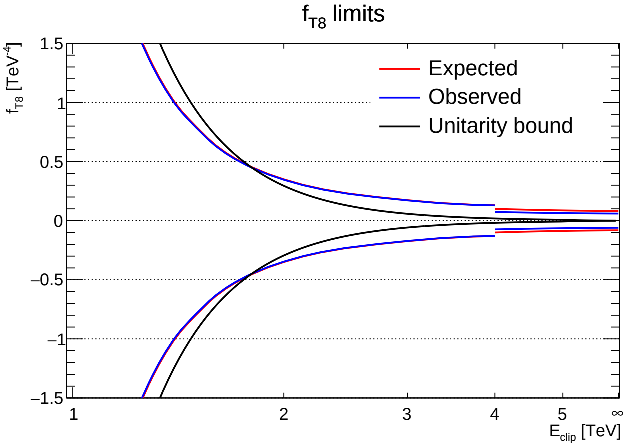

Non-unitarized limits.

Expected: [-0.081; 0.081] TeV^{-4}.

Observed: [-0.060; 0.060] TeV^{-4}.

Unitarized limits.

$E_{\text{clip}} = 1.7$ TeV.

Expected: [-0.53; 0.53] TeV^{-4}.

Observed: [-0.52; 0.52] TeV^{-4}.

Results for f_{T9}

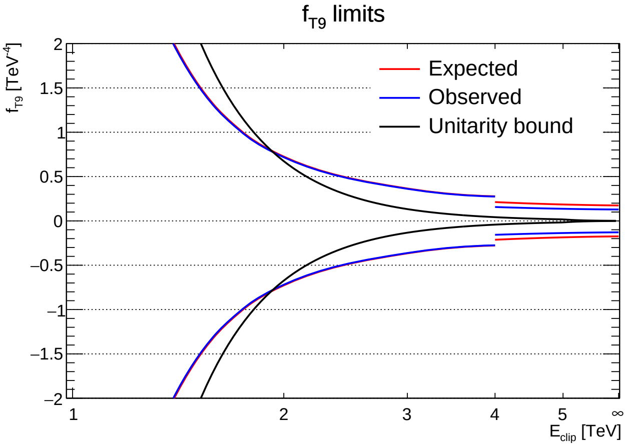

Non-unitarized limits.

Expected: [-0.17; 0.17] TeV^{-4}.

Observed: [-0.13; 0.13] TeV^{-4}.

Unitarized limits.

$E_{clip} = 1.9$ TeV.

Expected: [-0.81; 0.81] TeV^{-4}.

Observed: [-0.81; 0.80] TeV^{-4}.

f_{M0} optimization [1]

$E_{\mathbf{clip}}$, TeV	∞	5	4	3	2
p_T^γ>150 GeV	[-25; 25]	[-25; 26]	[-26; 27]	[-30; 30]	[-42; 43]
p_T^γ>300 GeV	[-14; 14]	[-14; 15]	[-15; 15]	[-17; 18]	[-25; 26]
p_T^γ>400 GeV	[-10; 11]	[-11; 11]	[-11; 11]	[-13; 13]	[-19; 20]
p_T^γ>500 GeV	[-8.7; 8.8]	[-8.9; 9]	[-9.3; 9.4]	[-11; 11]	[-17; 17]
p_T^γ>600 GeV	[-7.6; 7.7]	[-7.8; 7.8]	[-8.2; 8.3]	[-9.7; 9.8]	[-16; 16]
p_T^γ>700 GeV	[-7; 7]	[-7.1; 7.2]	[-7.6; 7.6]	[-9.2; 9.3]	[-17; 17]
p_T^γ>800 GeV	[-6.5; 6.5]	[-6.7; 6.7]	[-7.2; 7.2]	[-9; 9]	[-19; 19]
p_T^γ>900 GeV	[-6.3; 6.3]	[-6.5; 6.5]	[-7; 7]	[-9.2; 9.2]	[-23; 23]
p_T^γ>1000 GeV	[-6.5; 6.5]	[-6.7; 6.7]	[-7.4; 7.4]	[-10; 10]	[-31; 31]
p_T^γ>1100 GeV	[-6.7; 6.7]	[-7; 7]	[-7.8; 7.8]	[-11; 11]	[-39; 39]
p_T^γ>1200 GeV	[-6.9; 6.9]	[-7.2; 7.2]	[-8.3; 8.3]	[-13; 13]	
p_T^γ>1300 GeV	[-7.8; 7.8]	[-8.3; 8.3]	[-9.8; 9.8]	[-18; 18]	
Bound	[-0; 0]	[-0.066; 0.066]	[-0.16; 0.16]	[-0.51; 0.51]	[-2.6; 2.6]

f_{M0} optimization [2]

E_{clip}, TeV	1.5	1	0.9	0.8	0.7	0.6
p_T^γ>150 GeV	[-59; 61]	[-110; 120]	[-130; 140]	[-160; 170]	[-200; 210]	[-270; 280]
p_T^γ>300 GeV	[-36; 38]	[-74; 77]	[-92; 95]	[-120; 120]	[-160; 160]	[-220; 220]
p_T^γ>400 GeV	[-29; 30]	[-67; 68]	[-85; 85]	[-110; 110]	[-140; 140]	[-190; 190]
p_T^γ>500 GeV	[-28; 28]	[-70; 70]	[-88; 87]	[-110; 110]	[-140; 140]	[-190; 190]
p_T^γ>600 GeV	[-29; 29]	[-77; 77]	[-92; 92]	[-120; 120]	[-150; 150]	[-210; 210]
p_T^γ>700 GeV	[-35; 35]	[-85; 85]	[-100; 100]	[-140; 140]	[-180; 180]	[-260; 260]
p_T^γ>800 GeV	[-42; 42]	[-93; 93]	[-110; 120]	[-140; 140]	[-180; 180]	[-260; 260]
p_T^γ>900 GeV	[-47; 47]	[-110; 110]	[-140; 140]	[-170; 170]	[-250; 250]	[-400; 400]
p_T^γ>1000 GeV	[-58; 58]	[-140; 140]				
p_T^γ>1100 GeV						
p_T^γ>1200 GeV						
p_T^γ>1300 GeV						
Bound	[-8.1; 8.1]	[-41; 41]	[-63; 63]	[-100; 100]	[-170; 170]	[-320; 320]

Results for f_{M0}

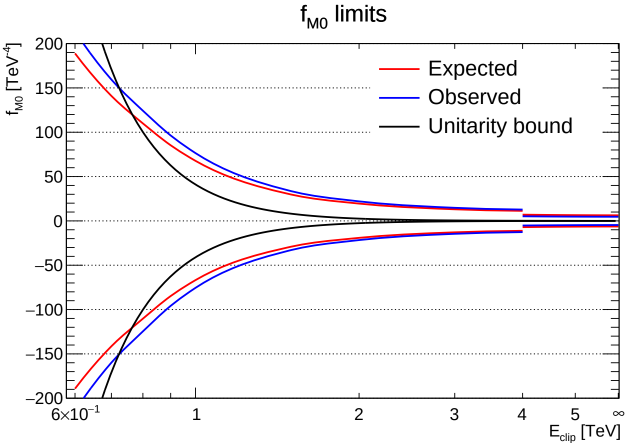

Non-unitarized limits.

Expected: [-6.3; 6.3] TeV^{-4}.

Observed: [-4.7; 4.7] TeV^{-4}.

Unitarized limits.

$E_{\text{clip}} = 0.7$ TeV.

Expected: [-140; 140] TeV^{-4}.

Observed: [-160; 160] TeV^{-4}.

Results for f_{M1}

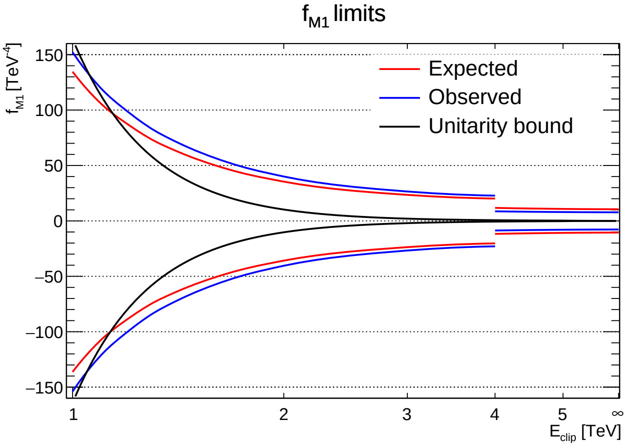

Non-unitarized limits.

Expected: [-11; 11] TeV^{-4}.

Observed: [-7.8; 7.8] TeV^{-4}.

Unitarized limits.

$E_{clip} = 1$ TeV.

Expected: [-140; 130] TeV^{-4}.

Observed: [-150; 150] TeV^{-4}.

Results for f_{M2}

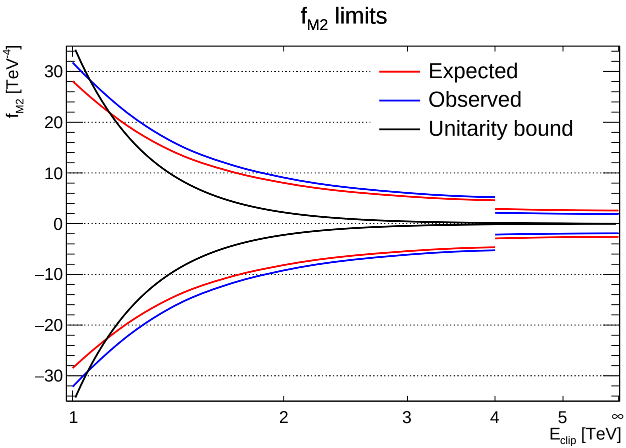

<u>Non-unitarized limits.</u>

Expected: [-2.6; 2.6] TeV^{-4}.

Observed: [-1.9; 1.9] TeV^{-4}.

<u>Unitarized limits.</u>

$E_{\text{clip}} = 1$ TeV.

Expected: [-28; 28] TeV^{-4}.

Observed: [-32; 32] TeV^{-4}.

Comparison: T-family

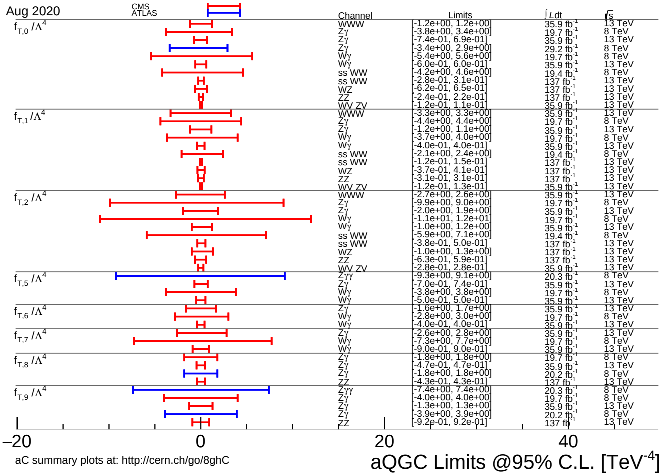

Coef.	Exp., TeV^{-4}	Obs., TeV^{-4}
f_{T0}	[-0.13; 0.12]	[-0.095; 0.085]
f_{T5}	[-0.12; 0.13]	[-0.89; 0.100]
f_{T8}	[-0.81; 0.81]	[-0.60; 0.60]
f_{T9}	[-0.17; 0.17]	[-0.13; 0.13]

Comparison: M-family

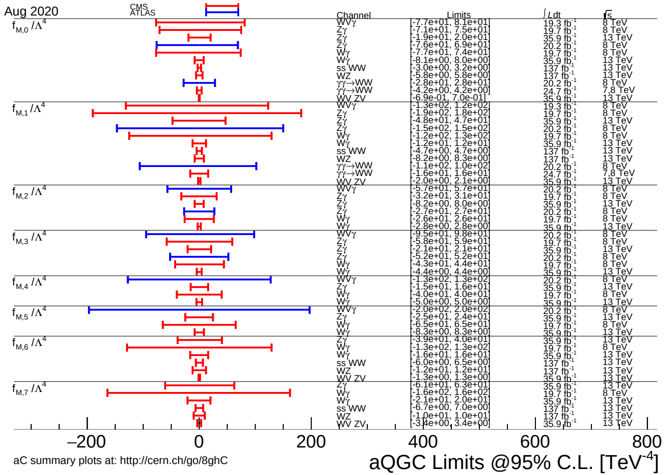

Coef.	Exp., TeV^{-4}	Obs., TeV^{-4}
f_{M0}	[-6.3; 6.3]	[-4.7; 4.7]
f_{M1}	[-11; 11]	[-7.8; 7.8]
f_{M2}	[-2.6; 2.6]	[-1.9; 1.9]

Theoretical linear limits

Coef.	f_{T0}	f_{T5}	f_{T8}	f_{T9}	f_{M0}	f_{M1}	f_{M2}
p_T^γ>150 GeV	-12.6, 0.8%	12.6, 0.8%	-1430, 5.5%	-1940, 4.6%	2130, 2.7%	-6950, 3.1%	-1060, 2.4%
p_T^γ>300 GeV	-3.92, 1.3%	3.91, 1.3%	-446, 5.8%	-585, 4.8%	1080, 4.4%	-3400, 4.9%	-526, 3.9%
p_T^γ>400 GeV	-2.11, 1.8%	2.11, 1.8%	-235, 6.3%	-311, 5.3%	878, 6.8%	-2830, 7.7%	-431, 6%
p_T^γ>500 GeV	-1.23, 2.7%	1.22, 2.7%	-132, 6.9%	-179, 6%	752, 10.5%	-2510, 12.3%	-386, 9.7%
p_T^γ>600 GeV	-0.773, 3.6%	0.765, 3.6%	-85.1, 8%	-118, 7.2%	651, 15.2%	-2820, 23.1%	-324, 13.5%
p_T^γ>700 GeV	-0.51, 5%	0.505, 5%	-54.8, 9.4%	-75.7, 8.5%	684, 25.9%	-2110, 28.2%	-353, 23.8%
p_T^γ>800 GeV	-0.355, 7.1%	0.353, 7%	-34.5, 10.7%	-53, 10.6%	993, 57.3%	-3070, 62.9%	-385, 39.1%
p_T^γ>900 GeV	-0.247, 9.4%	0.248, 9.4%	-22.6, 12.9%	-35.9, 12.9%	-4460, 395.9%	-5630, 184.4%	-296, 47.7%
p_T^γ>1000 GeV	-0.2, 11.9%	0.199, 11.9%	-17.6, 15.4%	-28, 15.5%	-904, 108.9%	2230, 100%	-341, 73.3%
p_T^γ>1100 GeV	-0.159, 16.5%	0.156, 16.5%	-12.9, 19.7%	-20.6, 19.7%			
p_T^γ>1200 GeV	-0.113, 24.8%	0.113, 24.8%	-9.25, 27.7%	-14.3, 27.6%			

Optimization for linear limits

Coef.	f_{T0}	f_{T5}	f_{T8}	f_{T9}	f_{M0}	f_{M1}	f_{M2}
p_T^γ>150 GeV	[-10.2; 8.5]	[-8.5; 10.2]	[-1170; 970]	[-1600; 1300]	[-1400; 1700]	[-5600; 4700]	[-860; 710]
p_T^γ>300 GeV	[-3.7; 3.3]	[-3.3; 3.7]	[-420; 380]	[-550; 500]	[-910; 1010]	[-3200; 2900]	[-490; 450]
p_T^γ>400 GeV	[-2.0; 2.1]	[-2.1; 2.0]	[-230; 230]	[-300; 310]	[-870; 850]	[-2800; 2800]	[-420; 430]
p_T^γ>500 GeV	[-1.2; 1.7]	[-1.6; 1.2]	[-130; 180]	[-180; 240]	[-1030; 750]	[-2500; 3500]	[-390; 530]
p_T^γ>600 GeV	[-0.77; 1.46]	[-1.44; 0.77]	[-85; 162]	[-120; 220]			
p_T^γ>700 GeV	[-0.51; 1.40]	[-1.38; 0.51]	[-55; 151]	[-76; 209]			
p_T^γ>800 GeV	[-0.36; 1.38]	[-1.37; 0.35]	[-35; 136]	[-53; 208]			
p_T^γ>900 GeV	[-0.25; 1.47]	[-1.48; 0.25]	[-23; 136]	[-36; 217]			
p_T^γ>1000 GeV	[-0.20; 1.74]	[-1.74; 0.20]	[-18; 155]	[-28; 247]			
p_T^γ>1100 GeV	[-0.16; 2.10]	[-2.05; 0.16]	[-13; 172]	[-21; 274]			

Statistical treatment

Test statistic: $t_\mu = -2\ln\lambda(\mu)$.

$$\lambda(\mu) = \frac{L(f, \hat{\hat{\theta}}(f))}{L(\hat{f}, \hat{\theta})}$$ — likelihood ratio.

CL_{s+b} technique: confidence interval is region in the parameter-of-interest (μ) space, where

$$p_\mu = \int_{t_\mu^{obs}}^{\infty} f(t_\mu|\mu)\, dt_\mu > \alpha = 0.05.$$

In the large-sample limit distribution $f(t_\mu|\mu)$ converges to χ^2 distribution.

Setting 95% CL limits: $t_\mu = 3.84$.

For setting limits EFTfun is used.

Example: f_{T0}, $p_T^\gamma > 900$ GeV.